LUND UNIVERSITY

Capacity maximisation of a handheld MIMO terminal with adaptive matching in an indoor environment

Plicanic, Vanja; Vasilev, Ivaylo; Tian, Ruiyuan; Lau, Buon Kiong

V. Plicanic, I. Vasilev, R. Tian, and B. K. Lau, "On capacity maximisation of a handheld MIMO terminal with adaptive matching in an indoor environment," *Electron. Lett*., vol. 47, no. 16, pp. 900-901, Aug. 4, 2011.

On capacity maximisation of a handheld MIMO terminal with adaptive matching in an indoor environment

V. Plicanic, I. Vasilev, R. Tian and B. K. Lau

This letter reports the capacity performance of a handheld dual-band dual-antenna compact MIMO terminal, which utilizes uncoupled adaptive impedance matching for capacity maximisation. The capacity is evaluated at 0.825 GHz and 2.35 GHz in an indoor office environment. The results show that adaptive matching enhances capacity by up to 44% and 22% at the low and high frequency bands, respectively, relative to no matching. At the low band, the capacity gain is attributed to both increased received power and decreased channel eigenvalue dispersion, whereas at the high band, the capacity gain is only due to increased power.

Introduction: In recent years, there has been a growing interest to employ adaptive impedance matching in conventional single antenna mobile terminals. Apart from compensating for the detuning of an antenna caused by user proximity [1], adaptive matching also introduces a degree of frequency reconfigurability for covering an increasing number of operating bands [2]. However, even though there are several adaptive matching solutions in the market for single-antenna terminals, an efficient and cost-effective implementation continues to be challenging. Moreover, new cellular communication systems such as Long Term Evaluation (LTE) require the implementation of multiple antennas in compact terminals, in order to exploit the benefits of multiple-input multiple-output (MIMO) technology. This requirement further complicates the design of adaptive matching networks, since the antenna elements are strongly coupled electromagnetically and can suffer from high signal correlation and severe power loss, in addition to user influence. Furthermore, correlation also critically depends on the propagation environment.

1

Earlier studies have confirmed that uncoupled matching networks for multiple antennas (i.e. one matching network per antenna) can be used to enhance the capacity of closely-spaced half-wavelength dipole antennas in a given propagation environment (see [3] and references therein). In particular, the capacity improvement results from an optimal trade-off between received power and correlation. However, these studies are largely based on simulations and they consider neither user influence nor realistic terminal antennas. Therefore, the effectiveness of adaptive matching for multiple-antenna terminals is largely unexplored.

In this Letter, the potential MIMO capacity gain from adaptive matching is examined in the context of multiple-antenna terminal application. Specifically, the scattering (or S) parameters of the entire MIMO system setup are measured in an indoor office environment, with the terminal held by phantom hands. Ideal adaptive matching circuits are then added in post-processing. The main goal is to ascertain the best-case benefits of uncoupled adaptive matching and their underlying mechanisms.

Dual-antenna terminal: The terminal configuration (see Fig. 1a) comprises two compact dual-band inverted F antennas (0.8-0.85 GHz and 2.3-2.4 GHz at -6 dB reflection coefficient) of an identical design [4]. The two bands are representative of cellular communications. However, to avoid interference and licensing issues, they do not overlap with existing cellular and wireless LAN bands. The antenna volumes are each $51{\times}9{\times}9$ mm^3. The total volume of the prototype is $120{\times}60{\times}9$ mm^3. The antenna feed separation is 0.28 wavelength (λ) at 0.825 GHz and 0.8λ at 2.35 GHz. The measured antenna efficiencies are -4.6 dB and -4.3 dB at 0.825 GHz and -1.9 dB and -2 dB at 2.35 GHz. The antenna isolations are 5.5 dB and 21 dB at 0.825 GHz and 2.35 GHz, respectively. The measured envelope correlation of the antenna patterns is 0.35 at 0.825 GHz and 0.01 at 2.35 GHz.

MIMO channel measurements: The transmit (TX) antenna configuration comprises two identical wideband monopole-based antennas, spaced by λ at 0.8 GHz. The antenna ground planes are positioned vertically at the height of 1.85 m. The dual-antenna terminal at the receive (RX) side was placed on a trolley at the height of 0.95 m, to replicate its height when held by a user in a standing posture. Moreover, it is held in a two-hand grip position (TH) by two IndexSAR hand phantoms, which mimics a common grip for data communication (see Fig. 1b). For reference purposes, the free space (FS) case (i.e. without user) is also evaluated at the same height.

The full four-port S-parameter representation of the 2×2 MIMO channel was obtained at the two bands of 0.8-0.85 GHz and 2.3-2.4 GHz (with a resolution of 5 kHz) with a four-port vector network analyzer (Agilent ENA 5017C). The intermediate frequency bandwidth (IFBW) was set to 2 kHz and an averaging of 20 snapshots was applied.

The measured indoor environment is a corridor, along with offices at both sides. With the TX kept at the same position, two propagation scenarios were considered: non-line-of-sight (NLOS) and line-of-sight (LOS). In NLOS, 5 RX locations were chosen in 5 rooms along both sides of the corridor, whereas in LOS, 5 RX locations were measured along the length of the corridor. At each location, 9 positions separated by λ at 0.8 GHz (arranged in a rectangular grid) and two orientations per grid position were measured to obtain good fading statistics [5]. Overall, there are in total 5×9×2 = 90 channel realizations in the space domain for each propagation scenario.

Capacity evaluation with adaptive matching: The capacity of the measured 2×2 MIMO channel is evaluated, assuming equal TX power allocation. In order to make fair comparisons between the FS and TH cases, as well as between no matching and

capacity-optimal matching, the MIMO channels from all cases are normalised with the average channel gain of a common reference [5], i.e. FS case with no matching, at each RX location. A common reference enables the comparison to account for differences in both received power and eigenvalue dispersion (ED). ED measures the scattering richness of a channel, with lower ED indicating greater richness. To minimise the impact of channel estimation error in the capacity calculation, the reference SNR is set to be 10 dB. This is such that the measured average SNR for each case is at least 10 dB higher than the evaluation SNR. At each frequency band, 10 MHz of bandwidth around the centre frequencies is used. As a further reference, the capacity of the ideal 2×2 i.i.d. Rayleigh case is also calculated.

To obtain the capacity-optimal uncoupled matching states for each normalised instantaneous channel realization, a dense grid of impedance matching states on the Smith chart is applied to each of the two antenna ports in the RX configuration. The capacity with all possible matching states across the two ports is then calculated using the procedure detailed in [6]. Since the matching is performed at the centre frequency only, the matching states at the two antenna ports that maximise the capacity at that frequency are then applied to the full 10 MHz bandwidth.

Results and discussion: The capacity performances with and without matching in the NLOS scenario are depicted with cumulative distribution functions (CDFs) in Fig. 2 and Fig. 3, at 0.825 GHz and 2.35 GHz, respectively. At 0.825 GHz, it is observed that optimal matching for the TH case enables a large capacity enhancement of 44% at 50% outage probability, relative to no matching. At 2.35 GHz, the improvement is 22%. Similar improvements are achieved for the LOS scenario with optimal matching, and hence the LOS results are omitted here for the sake of conciseness.

The underlying mechanisms of the achieved capacity gain can be explained in terms of variations in received power and ED, as given in Table 1. Due to rich scattering in the measured indoor environment, it is assumed that the ED variation can be translated as SNR variation, as suggested in [7]. At 0.825 GHz, the capacity gain in the TH case results from the increased received power and ED gain, with power gain being the dominant contributor (see Table 1). The matching states that maximise the capacity reflect a trade-off between maximum power transfer and maximum channel richness, where the maximum power transfer corresponds to the conjugate matching of the antenna input impedances. At 2.35 GHz, the capacity gain comes almost entirely from conjugate impedance matching for maximum power transfer. Hence, little or no ED gain is observed in Table 1. Contrary to 0.825 GHz, the ED is not significantly affected by the hands in the TH case as compared to the FS case. The lower ED at 0.825 GHz in the handheld mode is related to the high correlation between the two closely-spaced antennas, which is significantly influenced by the hands, due to the entire chassis acting as the antenna [8]. On the other hand, at 2.35 GHz, the antenna performances are far more affected by the absorption in the hands, which results in a lower power gain with adaptive matching than that at 0.825 GHz.

Conclusions: In this work, uncoupled adaptive matching is practically demonstrated to be a promising technique for improving the capacity performance of MIMO terminals. In NLOS office environment, the measured capacity gains, relative to no matching, are observed up to 44% and 22% at low and high frequencies, respectively. At 0.825 GHz, the capacity gain comes from the combined effect of higher received power and lower ED. At 2.35 GHz, the received power alone provides the capacity improvement. Further work is required to study the impact of real (i.e. lossy) matching networks on the achievable capacity gains.

References

1 RAMACHANDRAN P., MILOSAVLJEVIC Z., and BECKMAN C.: 'Adaptive matching circuitry for compensation of finger effect on handset antennas'. In Proc. 3rd European Conf. on Ant. and Propag. EuCAP 2009, Berlin, pp. 801-804.

2 HU Z.H., DONG C.T.P., KELLY J., HALL P.S., GARDNER P.: 'Wide tunable dual-band reconfigurable antenna', Electron. Lett., 2009, 45 (22), pp.1109-1110.

3 JENSEN M. A., AND LAU B.K.: 'Uncoupled matching for active and passive impedances of coupled arrays in MIMO systems', IEEE Trans. on Ant. and Propag., 2010, 58 (10), pp. 3336-3343.

4 Patent, Pub. No. WO/2007/049414: 'Multiband antenna device and communication terminal device', SONY ERICSSON MOBILE COMMUNICATIONS, JAPAN.

5 TIAN R., PLICANIC V., LAU B.K., and YING, Z.: 'A compact six-port dielectric resonator antenna array: MIMO channel measurements and performance analysis', IEEE Trans. on Ant. and Propag., 2010, 58 (4), pp. 1369-1379.

6 WALLACE, J.W., and JENSEN, M.A.: 'Mutual coupling in MIMO wireless systems: A rigorous network theory analysis', IEEE Trans. on Wireless Commun., 2004, 3 (4), pp. 1317-1325.

7 SUVIKUNNAS P., SALO J., VUOKKO L., KIVINEN J., SULONEN K., and VAINIKAINEN P., 'Comparison of MIMO antenna configurations: methods and experimental results', IEEE Trans. Veh. Technol., 2008, 57 (2).

8 PLICANIC V., LAU B.K., DERNERYD A., and YING, Z.: 'Actual diversity performance of a multiband diversity antenna with hand and head effects', IEEE Trans. on Ant. and Propag., 2009, 57 (5), pp. 1547-1556.

Authors' affiliations:

V. Plicanic (Sony Ericsson Mobile Communications AB, SE-221 80 Lund, Sweden and Department of Electrical and Information Technology, Lund University, SE-221 00 Lund, Sweden)

E-mail: vanja.plicanic@sonyericsson.com

I. Vasilev, R. Tian and B. K. Lau (Department of Electrical and Information Technology, Lund University, SE-221 00 Lund, Sweden)

Figure captions:

Fig. 1 (a) Design of the dual-antenna prototype (b) Dual-antenna prototype in two hand grip position

Fig. 2 CDFs of measured capacities before and after adaptive matching is applied, for FS and TH cases in NLOS at 0.825 GHz.

Black curves: TH user case
Grey curves: FS case

Fig. 3 CDFs of measured capacities before and after adaptive matching is applied, for FS and TH cases in NLOS at 2.35 GHz.

Black curves: TH user case
Grey curves: FS case

Table captions:

Table 1 Gain in received power, ED and capacity at 50% outage probability due to uncoupled adaptive matching for TH and FS cases in NLOS.

Figure 1
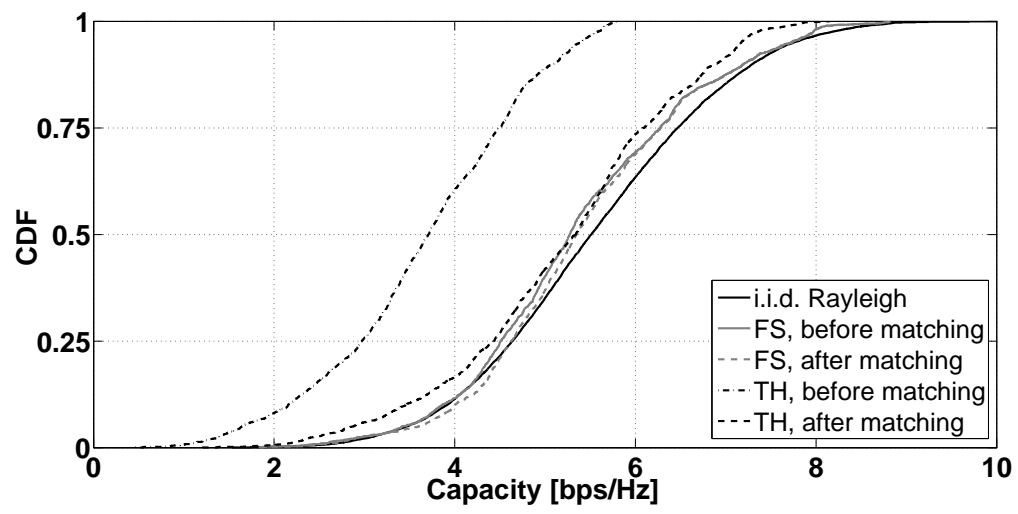

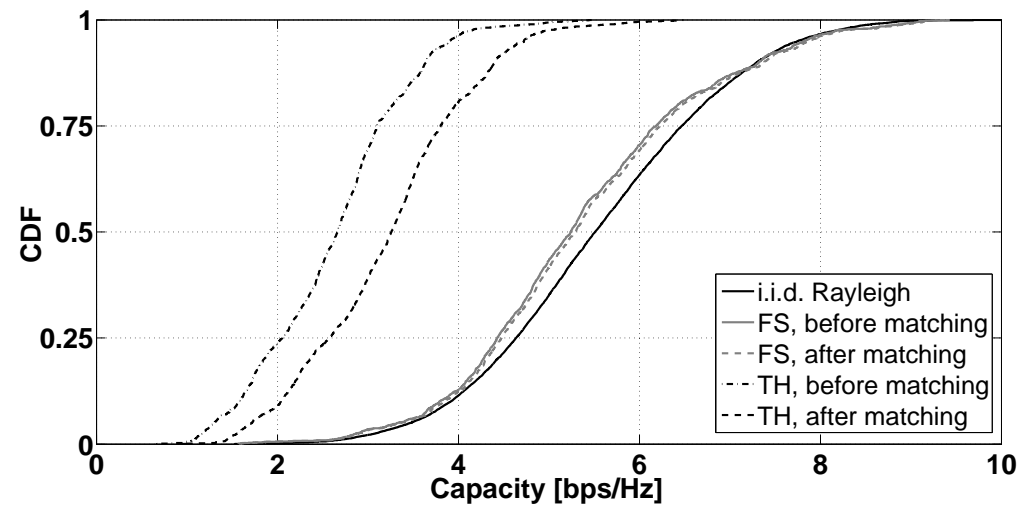a   b

Figure 2

Figure 3

Table 1

Frequency [GHz]	User case	Power gain [dB]	ED gain [dB]	Capacity gain [%]
0.825	FS	0.67	-0.65	0.01
	TH	3.61	0.82	44
2.35	FS	0.11	-0.01	0.01
	TH	1.71	0.02	22